



Testing Water Yield, Efficiency of Different Meshes and Water Quality with a Novel Fog Collector for High Wind Speeds

Christian Schunk^{1*}, Peter Trautwein², Herbert Hruschka², Ernst Frost², Leslie Dodson³, Aissa Derhem⁴, Jamila Bargach⁴, Annette Menzel^{1,5}

¹ *Ecoclimatology, Technische Universität München, 85354 Freising, Germany*

² *Water Foundation, 82067 Ebenhausen, Germany*

³ *Worcester Polytechnic Institute, Worcester, MA 01609, USA*

⁴ *Association Dar Si Hmad, Agadir 80 000, Morocco*

⁵ *Institute for Advanced Study, Technische Universität München, 85748 Garching, Germany*

ABSTRACT

Fog harvesting techniques for water collection have been implemented successfully worldwide for several decades. However, at locations with high wind speeds, traditional installations require high maintenance efforts endangering the sustainability of projects. Furthermore, the efficiency of fog collection meshes and the water quality in the field are key questions for the implementation of large-scale facilities. This study presents a novel, durable fog collector design and investigates the yield (fog + rain) and inorganic water quality of different potential collection meshes at a test site in Morocco. The pilot facility proved very reliable with only minimal maintenance required. Rankings of the efficiency of different fog nets were set up, with monofilaments and three-dimensional structures tending to show higher yields than woven fabrics such as the traditional ‘Raschel’ mesh. However, differences from fog event to fog event could be identified. Water quality was better than that of local wells and met WHO guidelines, except for the ‘first flush’ just after the start of fog events.

Keywords: Fog collection; Mesh; Collector; Water quality.

INTRODUCTION

Fog collection is a passive and potentially low cost method to generate water in areas with frequent fog occurrence and otherwise scarce or low quality water supply (Domen *et al.*, 2014; Abdul-Wahab *et al.*, 2007a). A review of the wide range of exploratory studies and fog collection projects worldwide can be found in Klemm *et al.* (2012). In addition, Sontag and Saylor (2016) propose using a very similar technology for reducing the water loss in thermoelectric power plants.

Typically, meshes are used to intercept fog droplets, which accumulate over time at the filaments until gravity is sufficient to move them down into gutters and subsequent storage or distribution facilities. A widely used setup includes the food safe, polyethylene Raschel mesh (Klemm *et al.*, 2012) that is suspended from the frame or poles of so-called standard (Schemenauer and Cereceda, 1994a) or large

(Schemenauer and Cereceda, 1994b) fog collectors (SFC and LFC, respectively). While the first are meant for exploratory studies using a 1.00 m² surface area, the LFCs are intended for larger-scale fog collection projects and essentially consist of two vertical poles anchored to the ground by foundations and additional steel cables. The Raschel mesh is stretched out between those, supported by steel or other cables on the edges while plastic gutters are used to collect the harvested water (Schemenauer and Cereceda, 1994b). The meshes are mounted in a ‘landscape’ orientation with a surface area of up to 50 m² (Schemenauer and Cereceda, 1994b), depending on local conditions. The collection efficiency of the Raschel mesh in a LFC has been investigated by Schemenauer and Joe (1989) and was found to depend on the wind speed. While this setup has been successfully implemented in many regions of the world (cf. Klemm *et al.*, 2012), there have been a number of attempts to improve it or to find superior fog collection meshes.

Novel meshes have been developed in a large number of recent studies, often including biomimetic aspects such as the hydrophilic-hydrophobic structure found on the Namib desert beetle (e.g., Parker and Lawrence, 2001; Wang *et al.*, 2015, Wang *et al.*, 2016; Zhu *et al.*, 2016), the structure of plants (e.g., Cao *et al.*, 2014; Heng *et al.*, 2014; Ju *et al.*,

*Corresponding author.

Tel.: 49-8161-71-4745; Fax: 49-8161-71-4753

E-mail address: schunk@wzw.tum.de

2014; Azad *et al.*, 2015a, b; Bai *et al.*, 2015; Tan *et al.*, 2016), spider silk (e.g., Zheng *et al.*, 2010; Dong *et al.*, 2016) and other bioinspired materials (e.g., Heng and Luo, 2014). A recent review can be found in Zhu and Guo (2016). Hydrodynamic models can be used to derive efficiency ratings for different processes involved in fog collection (e.g., fog interception efficiency, aerodynamic collection efficiency, capture efficiency (Rivera, 2011)) and may also lead to improved materials or arrangements. The study of Park *et al.* (2013) is an example for optimizing meshes at the laboratory scale with the help of a combined hydrodynamic and surface wettability model. Field tests of different materials are rather scarce and were performed by Shanyengana *et al.* (2003), Abdul-Wahab *et al.* (2007b), Fernandez *et al.* (2016) and Feld *et al.* (2016). While both Shanyengana *et al.* (2003) and Fernandez *et al.* (2016) found generally higher yields for the Raschel mesh than for alternate materials, a significant number of intervals is described in Fernandez *et al.* (2016) during which the alternate mesh collected water while the Raschel mesh did not. Feld *et al.* (2016) report that the Enkamat 7220 and 7010 turf reinforcement mats outperformed the Raschel mesh by 62% to 146% and 75% to 178% at different sites, respectively.

In order to improve the water yield and economic competitiveness, Lummerich and Tiedemann (2011) tested three full-scale fog collectors in Peru and found highest yields for the ‘Eiffel’ type consisting of two separated layers of Raschel mesh with additional stripes in between. Apart from maximizing the potential yield, some studies tried to overcome problems in the durability of the LFCs fitted with Raschel meshes, as described in Holmes *et al.* (2015) and Rivera and Lopez-Garcia (2015). In particular, the Raschel mesh tends to sag in the wind, leading to water loss and mesh deformation, rupture at the attachment areas due to high load factors or within the mesh surface (Holmes *et al.*, 2015), which may be caused by abrasion of material, spots weakened during the mesh installation and cyclic loads/wind gusts (Rivera and Lopez-Garcia, 2015). Damages to the non-engineered LFCs themselves may include failures of the supporting structure or foundations (Rivera and Lopez-Garcia, 2015; Holmes *et al.*, 2015). All of these damage patterns have been observed by the authors of the present study at field sites in Boutmezguida, Morocco and Arborobue, Eritrea.

Rivera and Lopez-Garcia (2015) investigated the mechanical properties of the Raschel mesh, finding highest stiffness in the knitting direction and recommending an optimum mounting orientation (longitudinal direction aligned with the shortest dimension of the collector). They also inferred from a structural model that the mesh should be able to withstand steady wind speeds over 50 m s^{-1} , however indicating that other factors mentioned above may cause the mesh to fail at much lower wind speeds (Rivera and Lopez-Garcia, 2015). Based on these observations and numerical simulations, Holmes *et al.* (2015) propose a novel modular-funnel large fog collector (MF-LFC) featuring a three-dimensional arrangement of the meshes and support structures, an oblique angle of incidence between wind and

mesh, and a small mesh area between the supporting frames.

In addition to the efficiency and durability of fog collectors and associated meshes, the quality of the collected fog water is a critical factor determining the possible subsequent water use. Although fog water generally has higher soluble concentrations than rainwater (Klemm *et al.*, 2012), studies in the Namib desert (Shanyengana *et al.*, 2002), the Asir region in Saudi Arabia (Gandhidasan and Abualhamayel, 2012) and the Dhofar region in Oman (Abdul-Wahab *et al.*, 2007b) showed the ion concentrations in water obtained from fog collection projects to be within the WHO guidelines for drinking-water quality. However, Schemenauer and Cereceda (1992) found extremely low pH values in fog water from the El Tofo site in Chile. While in their study, ion and trace element concentrations were generally acceptable, Sträter *et al.* (2010) later additionally found high sulfate concentrations and heavy metal enrichment factors at another Chilean site. Their analysis suggests that even for a remote site, the water quality may be influenced by far-away emission sources, which are passed by the air masses before reaching the collection site. Both Schemenauer and Cereceda (1992) and Sträter *et al.* (2010) found that deposition on the fog collection meshes during periods without fog leads to an initial ‘first flush’ of highly polluted fog water. They also state that collected fog water quality after this first flush depends on the collector material as well as on the incoming fog (Schemenauer and Cereceda, 1992) and that fog water quality should be verified on a regular basis before it is used for domestic purposes (Sträter *et al.*, 2010).

The present paper presents a novel fog collector design for enhanced durability in high wind speeds and aims to compare the water yield and quality of 11 different meshes as well as two support grids at Boutmezguida, Morocco in the period November 2013 to June 2015.

METHODS

Fog Collector Design

The novel fog collector (cf. Fig. 1) consists of an anchored frame construction made of galvanized steel pipes (diameter 114.3 mm for vertical and 88.9 mm for horizontal pipes, respectively; wall thickness 4 mm) and stainless steel ropes attached to concrete foundations and pegs, respectively. Vertical fog collection meshes (height 4.5 m, width 2.0 m) mounted on support grids are attached using flexible rubber expanders. Both the anchoring of the frame construction as well as the expanders provide some flexibility for high wind speeds and gusts. The expanders also work as predetermined breaking points and are easy to replace in case of overloading, while the main structure remains intact. Plastic gutters are integrated in the lower mesh mounting system and multiple frames can be linked to minimize the cost of materials. A more detailed description can be found in Wasserstiftung (2015).

Study Site and Pilot Facility

A pilot facility was set up at the Boutmezguida fog collection site (29°12'30"N; 10°01'30"W) in Morocco. It is

located approximately 130 km south of Agadir and 20 km inland from the Atlantic Ocean, near the summit of a 1,225 m high mountain (cf. Fig. 2). The area is extremely arid but characterized by frequent fog events linked to the cold Canary current and the rising terrain. Marzol and Megía (2008) and Marzol *et al.* (2011) analyzed the basic meteorological conditions, social aspects and fog collection potential, reporting a total of 552 (33%) of fog days in their study period (2006–2010), of which 12% (66) were influenced by rain. The average yield was reported as $10.6 \text{ l m}^{-2} \text{ d}^{-1}$ (fog + rain) and $8.7 \text{ l m}^{-2} \text{ d}^{-1}$ (fog only) (Marzol *et al.*, 2011). An array of 20 LFCs (600 m^2 total mesh area) was installed in 2006, which however required frequent maintenance due to wind damages ranging from torn

meshes to bent support poles. An overview of all activities at the study site and their social impacts can be found in Dodson and Bargach (2015).

The novel pilot facility set up for this study consists of six segments of the fog collector as described above, which were mounted in a line perpendicular to the main wind direction in fog events. The yield of each individual mesh was measured using a 100 ml tipping-bucket counter (KIPP-100, UMS AG), which also provided a sampling system to divert 2.5% of the flow to a sampling bottle. Additionally, air temperature, relative humidity, precipitation, surface wetness, wind speed and wind direction were recorded every 5 min with instrumentation by Decagon, Inc. The tipping-bucket rain gauge was observed to also



Fig. 1. Photograph of the pilot facility representing the novel fog collector design. Positions 1 through 6 are in sequence from left to right. Positions 1 & 6 are named outside, 2 & 5 middle and 3 & 4 inside. A previously used version of the large fog collector (LFC) can be seen at the left edge of the image.

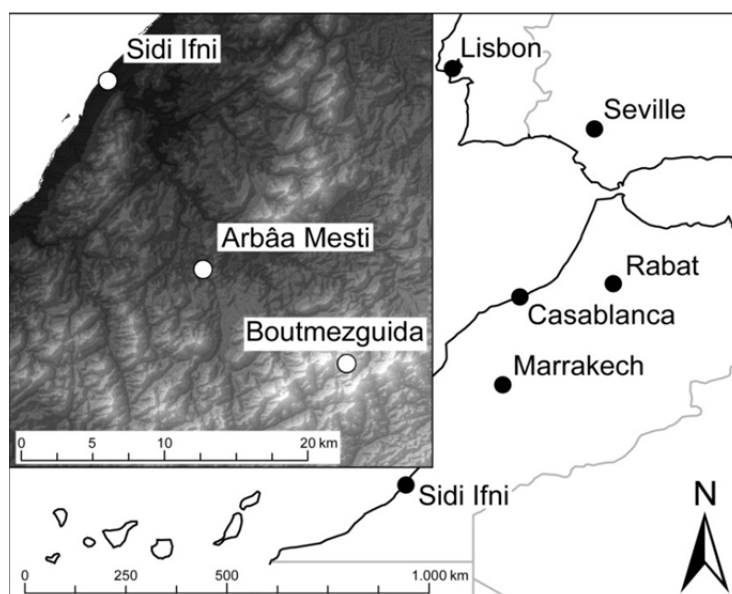


Fig. 2. Location of the pilot facility at Boutmezguida, Morocco.

capture a significant amount of fog during high-intensity fog events, leading to an overestimation of both days with and amount of precipitation. Thus, its values could not be used to determine rain-free fog events and fog+rain yield had to be used in the main analysis. To show at least a rough estimate of the potential influence of rain, synoptical observations and precipitation at the two nearest standard meteorological stations Sidi Ifni and Guelmim (23 and 25 km air-line distance and 1,200 and 920 m lower than the measurement site, respectively) were employed. Their measurements and observations were available as three-hourly and hourly values during the daytime, respectively, whereas nighttime observations and measurements (18:00 to 6:00 h LST) were present as twelve-hourly values.

Fog Collection Meshes and Supporting Grids

A total of 11 different fog collection meshes and two supporting grids were used within the 19-month experimental phase (November 2013 until June 2015, cf. Table 2), including woven fabrics (Shade and Raschel nets), monofilaments (e.g., Hail net, Antigranizio and Mosquitera), as well as three dimensional structures (Enkamat, Spacer fabric, Slubbed fabric) and a dual set of Hail nets with a separation of ≈ 115 mm. The Raschel mesh was used in a double layer as prescribed by Schemenauer and Cereceda (1994a); the same was done with the Hail net, except for the leeward part of the dual set configuration. In addition to plastic nets, two stainless steel meshes were tested. All materials and their properties, including shade coefficient determined from digital images, are shown in Table 1. In contrast to previous systems, where the fog collection mesh itself was suspended from the supporting structure, meshes in this study were mounted on two different, rigid supporting grids using cable ties, except for the stainless steel nets.

Mesh Test Procedures

The pilot facility was installed in November 2013 and has remained in operation till to date. This publication is based on two test phases (test phase 1: November 27, 2013 until October 14, 2014 and test phase 2: November 4, 2014 until June 25, 2015). In test phase 1, the collector was equipped with six different meshes (Shade net, Raschel net, Slubbed fabric, Enkamat, Hail net, Spacer fabric) all mounted on supporting grid 1. As there may be an influence of the linear setup on the yield at each position (expected lower wind speeds and thus lower yield at the center of the fog collector), the arrangement of the meshes was changed on two occasions during the test phase, so that all meshes were equally placed in the outside, middle and inside positions of the collector (cf. Fig. 1). The assignment of each mesh and position in the sub-periods can be found in Table 2.

In test phase 2, the choice of meshes was optimized with the results from the previous phase and supporting grid 2 was used. The mesh positions were again changed twice, however, two meshes (Enkamat and Mosquitera) were replaced by two other ones (Stainless steel 1.5×5 and Stainless steel 3×5) during this phase. This meant that not

all of the meshes could be assigned to each position in the same way as in test phase 1 (cf. Table 2), as some of them were not used during the entire three sub-periods defined by the change of mesh positions. During both test phases, the fog collector and measuring system were regularly inspected by local staff.



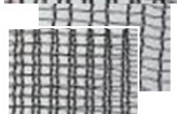

Data Preparation and Analysis

The raw fog yield data (number of tips of the 100 mL tipping-buckets per 5-minute intervals) were consistency-checked by manually comparing all tipping-bucket counter values for each individual day in the test periods. In the case of malfunctions (typically blockage of tipping-bucket counters by sand), data from the non-operational device(s) were discarded. All remaining raw data were converted into liters per square meter of mesh surface area and aggregated for each fog event, using a period of ≥ 30 minutes without any tips to partition individual events. While we consider this as the most generic way of reporting fog yield data (since fog and meteorological conditions tend to change from event to event rather than from day to day), daily sums of yield are also reported for comparability with previous studies. Since the precise definition of these 24-hour periods is not specified in most of the literature (e.g., Schemenauer and Cereceda, 1994a; Shanyengana *et al.*, 2002; Marzol *et al.*, 2011), the most conventional definition of a day, ranging from midnight to midnight has been used. However, as fog occurs primarily at night and may in some cases last longer than 24 hours, single fog events may thus be split into two or more days. To give an overview of the data, histograms of the mean yield of all operational meshes per event and per day (Fig. 3), as well as time series plots of the yield and selected meteorological parameters (supplementary material) are shown.

As mentioned in the description of the study site and pilot facility, precipitation data measured near the pilot facility proved to be unreliable and could thus not be used to reliably exclude fog events influenced by rain from the analysis. For additional reference, the number of fog events occurring during or outside of rain events at two nearby standard meteorological stations is shown in Fig. 3. As these stations are too far away from the pilot facility to accurately reflect the conditions there, all yield data reported here are not filtered for rain occurrence and thus represent the fog + rain yield.

In order to determine the influence of mesh type and mesh position on yield, linear models were employed. These were used to determine the differences between mesh type dependent on fog intensity, defined as the mean (fog + rain) yield over all operational nets, and to determine the influence of mesh position. This modelling approach was chosen over simple descriptive statistics such as boxplots, mainly for three reasons. First, while in test phase 1 all nets were mounted during all sub-periods, in test phase 2 nets were exchanged and not all nets were mounted at the same time; in addition, there were rather frequent failures/blockages of the measuring devices so that even during test phase 1, not all mesh yields could be measured for each individual fog event/day. Since fog events vary by time, not having

Table 1. Meshes investigated in this study and their properties. Shade coefficient was determined from digital images of the meshes. *Two layers of mesh measured; **single mesh layer used in second tier of the dual set.

Name	Trade name	Manufacturer/distributor	Material	Shape	Type	Shade coeff.	Image
Antigranizio	Antigranizio 5 × 4	TW Technical Textiles GmbH, D-Weyarn	HDPE	2 D	mono-filament	30%	
Enkamat	Enkamat® 7220	Colbond GmbH & Co. KG, D-Obernburg	PA6	3 D	mono-filament	67%	
Hail net	Austronet 241	Plaspack Netze GmbH, A-Schwanenstadt	HDPE	2 D	mono-filament	37%*	
Hail dual set	Austronet 241	Plaspack Netze GmbH, A-Schwanenstadt	HDPE	2 D, 2 tiers	mono-filament	37%* / 22%**	
Mosquitera	Mosquitera 6 × 6	TW Technical Textiles GmbH, D-Weyarn	HDPE	2 D	mono-filament	29%	
Raschel net	35% Raschel	Marienberg, CL-Santiago de Chile	PP	2 D	woven fabric	73%*	
Shade net	Austronet 202 UV	Plaspack Netze GmbH, A-Schwanenstadt	HDPE	2 D	woven fabric	54%	
Slubbed fabric	F-20200/14	Waterman Polyworks® GmbH, D-Horn-Bad Meinberg	PES	3 D	mono-filament	48%	
Spacer fabric	3DEA Abstands-gewirke	Essedea® GmbH & Co. KG, D-Wassenberg	PES	3 D	mono-filament	42%	
St. steel 1.5 × 5	custom made, gaps 1.5 × 5.0 mm	Dorstener Drahtwerke - H.W. Brune & Co. GmbH, D-Dorsten	Stainless steel	2 D	mono-filament	23%	
St. steel 3 × 5	custom made, gaps 3.0 × 5.0 mm	Dorstener Drahtwerke - H.W. Brune & Co. GmbH, D-Dorsten	Stainless steel	2 D	mono-filament	18%	
Supporting grid 1	Terram TurfProtecta®	Fiberweb Geo GmbH, D-Leipzig	HDPE	2 D	supporting grid	29%	
Supporting grid 2	TriAx®	Tensar® International GmbH, D-Bonn	HDPE	2 D	supporting grid	25%	

all nets at all sub-periods, events and days would induce bias if not standardized for the fog intensity. Nets with generally higher yields but tested in less foggy conditions could then be confounded with nets with generally lower yields but tested in more intense fog. Second, to determine the influence of net position, the same confounding can

occur if not standardized for fog intensity. Third, with a modelling approach, the different sub-periods can be analyzed in one model, while otherwise, each sub-period would need to be analyzed separately because of the abovementioned confounding effects. This leads to a higher sample size and thus increases statistical power.

Table 2. Arrangement of the meshes on the fog collector during the test phases and sub-periods.

Position 1 outside	Position 2 middle	Position 3 inside	Position 4 inside	Position 5 middle	Position 6 outside
<i>test phase 1, supporting grid 1</i>					
27 Nov 2013–19 Mar 2014					
Shade net	Raschel net	Slubbed fabric	Enkamat	Spacer fabric	Hail net
21 Mar 2014–28 May 2014					
Enkamat	Hail net	Spacer fabric	Raschel net	Shade net	Slubbed fabric
29 May 2014–14 Oct 2014					
Raschel net	Slubbed fabric	Shade net	Hail net	Enkamat	Spacer fabric
<i>test phase 2, supporting grid 2</i>					
04 Nov 2014–18 Feb 2015					
Hail net	Enkamat	Spacer fabric	Antigranizio	Mosquitera	Hail dual set
19 Feb 2015–30 Apr 2015					
Antigranizio	St. steel 3 × 5	Hail dual set	Hail net	St. steel 1.5 × 5	Spacer fabric
30 Apr 2015–25 Jun 2015					
St. steel 1.5 × 5	Spacer fabric	Hail net	Antigranizio	Hail dual set	St. steel 3 × 5

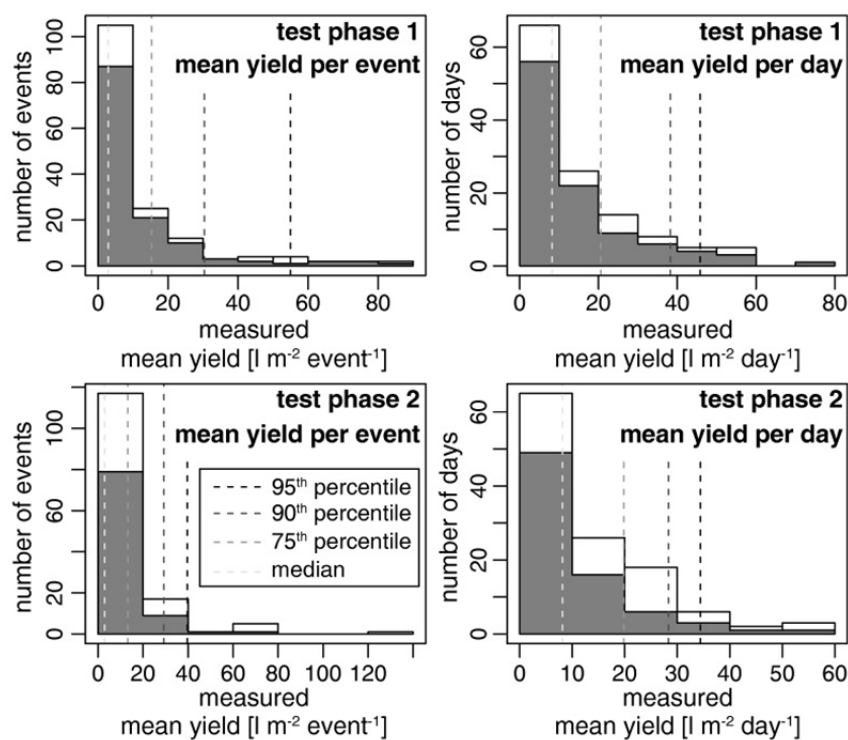


Fig. 3. Histograms of the mean (per event/day) fog (+rain) yield of all meshes for test phases 1 and 2, respectively. Overall bar height represents all measurements (including events/days with fog and rain); black areas are coarsely filtered for rain as described in methods. Vertical lines represent the median (50th), 75th, 90th and 95th percentile of mean fog + rain yield (calculated separately for all events/days and the two test phases), respectively, which are later used for determining the mesh position effect and the performance of individual meshes.

Fog + rain yield was the response variable and the explanatory variables included mesh type, mean yield over all meshes (fog + rain per event/day) and an interaction between the two to account for differences in fog (+rain) intensity and thus the non-linear distribution of fog (+rain) yield, as described above. To investigate the influence of the mesh position, an interaction between mean yield and the mesh position (outside, middle and inside, cf. Table 2) was added to one model. A symbolic representation of the

model including both interactions is shown in Eq. (1).

$$\sqrt{yield_{fog+rain}} = mesh \times \sqrt{\text{mean}(yield_{fog+rain})} + position \times \sqrt{\text{mean}(yield_{fog+rain})} \quad (1)$$

To ensure normality of the residuals, and thus be able to use a linear regression approach, fog (+rain) yield had to

be square-root transformed and the variance of the errors was modelled using an exponential function of $\sqrt{\text{mean}(\text{yield}_{\text{fog+rain}})}$, with different parameters per mesh.

The model was fitted using generalized least squares (gls function in R). Analysis of variance (ANOVA) as well as Akaike's Information Criterion (AIC) and the Bayesian information criterion (BIC) were used for model selection; post-hoc tests were used to derive significant differences between mesh types. Data processing and analysis were performed in R, version 3.1.1 (R Core Team, 2014) and packages “doBy” (Højsgaard *et al.*, 2013), nlme (Pinheiro *et al.*, 2017), plyr (Wickham, 2011) and lsmeans (Lenth, 2015).

Water Quality Procedures

Fog water samples were taken by trained personnel in two single fog events during test phase 1. The first flush was captured by directing the entire flow at the start of one fog event (after > 6 fog-free hours) into 250 mL sampling bottles until these were completely full (time depending on the yield and draining efficiency of each mesh). For steady-state samples, a sampling system integrated in the tipping-bucket counters described above was used during another single fog event that had already been under way. The sampling system diverted 2.5% of each mesh's overall flow into an attached sampling bottle and thus allowed for a longer integration time. The water was subsequently filled into new, single use, uncleaned but blank value-tested, sterile 250 mL polypropylene bottles and kept refrigerated, to be transported to Germany within a few days. Samples were not stabilized in the field to facilitate a speedy transport on passenger aircraft and were limited to one sample per mesh, due to weight restrictions. On arrival, they were brought to a laboratory immediately, where pH was measured electrometrically and they were stabilized to pH < 2 using nitric acid to be analyzed by inductively coupled plasma mass spectrometry (ICP-MS) for ions and heavy metals. Thus, all sample treatment and analysis procedures were carried out according to current German (DIN) and European (EN) standard test instructions for the relevant parameters. In addition, water samples of local wells were also taken and all measured values are compared to the WHO drinking-water guidelines (WHO, 2011).

RESULTS AND DISCUSSION

Fog Collector Durability

During both test phases with a total duration of 19 months, the fog collector and its meshes were intensively monitored both by the authors and local staff. In this period, only very minor damages occurred (e.g., single rubber expanders fallen off or stretched, supporting grids slightly deformed at the places where the expanders were attached). None of these had any effect on the stability and productivity of the collector structure and the meshes. Apart from exchanging the meshes and cleaning the tipping-bucket counters for the purpose of this study, maintenance tasks were thus minimal. There were no visible differences in the mechanical performance of the meshes, probably

due to the reinforcement by rigid supporting grids. It should be noted that during the study period, a large number of nearby LFC meshes were rendered inoperative, even despite vigilant maintenance.

Fog Events, Distribution of Yield Data and Comparison to Meteorological Parameters

Histograms of the mean yield both per event and per day for all meshes and the two test phases are shown in Fig. 3. Events/days likely influenced by precipitation (when precipitation was observed at one or both of the meteorological stations described above) are indicated as non-shaded parts of the histogram bars. Overall, there were 19% and 28% of likely rain-influenced events and 19% and 37% of likely rain-influenced days with fog in test phases 1 and 2, respectively. These numbers are higher than the 12% of fog days with rain reported by Marzol *et al.* (2011) and part of the reason for this may be the coarse temporal nighttime resolution of the meteorological observations (one value for 18:00 to 06:00 h LST each). Thus, rain occurring in this interval could not be assigned to one single day. The second test phase in particular was characterized by unusually frequent and intense (up to severe flooding in one single case in the end of November 2014) precipitation events. Fog events/days influenced by rain may partly explain the very high maximum (fog + rain) yields measured. However, there are also some very high yields that cannot be linked to precipitation as observed by the two nearby stations. This may be due to high spatio-temporal variability and orographically enhanced precipitation, indicating that the nearest available meteorological stations at ~24 km horizontal and > 1,000 m vertical distance (cf. above) may not be precise indicators of precipitation at the study site. It might, however, also be partially due to an increased collection efficiency of the unusually tall (6 m overall) pilot facility or the intense fog conditions at the study site. Since no robust measure of local precipitation is available, all further analyses are restricted to fog + rain yield. For both events and days, fog + rain yield data are highly positively skewed. The overall number of fog + rain events was 159 in test phase 1 and 141 in test phase 2, with a duration ranging from 5 minutes to > 4 days. Mean and median event duration was 9.7 and 5.3 hours, respectively, with a standard deviation of 11.5 hours. In both test phases, a total of 245 days with fog occurred (out of 554 days/44%). This is slightly higher than the 33% reported by Marzol *et al.* (2011) for the period 2006–2010 and may probably be explained by inter-annual variation. Vertical dashed lines in Fig. 3 indicate the median (50th), 75th, 90th and 95th percentile for fog + rain, which are later used for predicting the effects of the mesh position and different mesh types on yield, respectively. These percentiles were calculated separately for test phases 1 and 2.

While it was attempted to determine potential influences of meteorological conditions on fog yield, no meaningful results could be obtained by standard correlation/regression techniques. For a general overview, time-series plots of fog yield and selected meteorological parameters (temperature, relative humidity, wind speed and direction) are available

in supplementary Figs. S1 and S2 for test phases 1 and 2, respectively.

Effect of the Mesh Position on Yield

In order to investigate whether the (fog + rain) yield and thus the overall comparability of our data was influenced by the position of the meshes in the fog collector, data from test phase 1 was used, where each mesh was placed in each position. For this purpose, both interaction terms between mean yield per event (intensity) and mesh type, and between mean yield and the mesh positions were included in the linear model and predictions made for the median (50th), 75th, 90th and 95th percentiles of the mean yield per event or day. This model was also compared to a simpler one without the mean yield-mesh position interaction term using AIC and BIC. In the event-based assessment, a slight, gradual increase from the outside to middle to inside position is visible, while the daily aggregation shows the maximum yield at the middle position (Fig. 4). Considering the general understanding of the fog collection process and its relation to wind speed (cf. Schemenauer and Cereceda, 1994c; Bresci, 2002; Rivera, 2011), this is rather surprising since a gradual decline of wind speed and yield towards the center would have been expected. Differences but also confidence intervals are increasing for increasing yield levels in both cases. Although the mesh position is significant in the more complicated model at $p \leq 0.05$, its influence on yields was minor compared to fog intensity (mean yield), as well as to mesh type. For instance, for above average fog + rain yields (75th percentile), differences in yield due to position are up to 0.6 l m^{-2} both per event and day, while the differences in yields due to mesh type are up to 7.6 and 10.0 l m^{-2} per event and day, respectively (cf. Figs. 4 and 5).

Including the mesh position furthermore does not increase the model explanatory power (AIC -771.05 vs. -795.25 and BIC -662.48 vs. -705.48 for the events-based models; AIC -367.16 vs. -391.37 BIC -264.79 vs. -306.70 for the day-based models, respectively). Therefore, mesh position was omitted from further analysis.

Yield of the Different Meshes

Following the results of the previous section, the fog + rain yield of the different meshes is compared without considering the mesh position (linear model as in Eq. (1), however without the term $position \times \sqrt{\text{mean}(\text{yield}_{\text{fog+rain}})}$), using a post-hoc test with significance level 0.05 and p-values adjusted for multiple testing. Once more, the mesh effect is presented for the four percentiles previously used and results are compensated for the non-linear distribution of yields (i.e., fog intensity) by including the mean fog + rain yield of all nets per fog event/day in the model. Results thus obtained are shown in Fig. 5 with the different letters indicating significantly different yields between meshes at the respective fog (+rain) intensity (mean yield), represented by dashed lines. When considering these results, it should be noted that the days and events have not been filtered for situations influenced by rain. As the collection efficiency for fog and rain may be governed by different properties of the meshes, this may slightly affect the analysis. However, events and days potentially influenced by rain were relatively few (cf. above) and different intensities/mean yields not measured for all meshes (e.g., due to not all mesh types being mounted simultaneously, fog events that also included rain, or tipping-bucket counter malfunctions) are accounted for by our statistical approach.

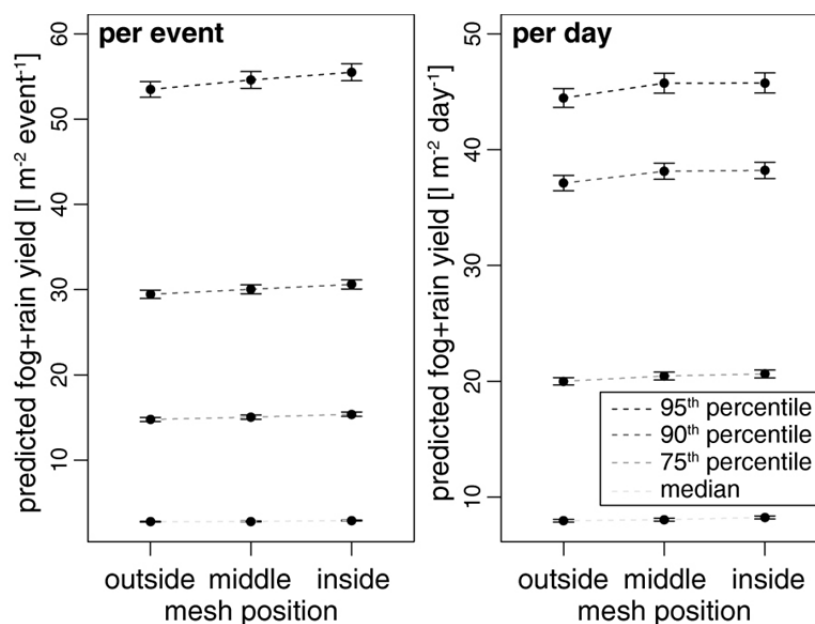


Fig. 4. Dependence of fog + rain yields on mesh positions. Shown are predicted values for yields for various levels of intensity (mean yield). For each position, the four points denote the expected yield under average conditions (median), under above average fog intensity (75th percentile), and under two extreme fog conditions denoted by the 90th and 95th percentiles. Results are based on linear modelling of fog + rain yields for test phase 1, see methods for details.

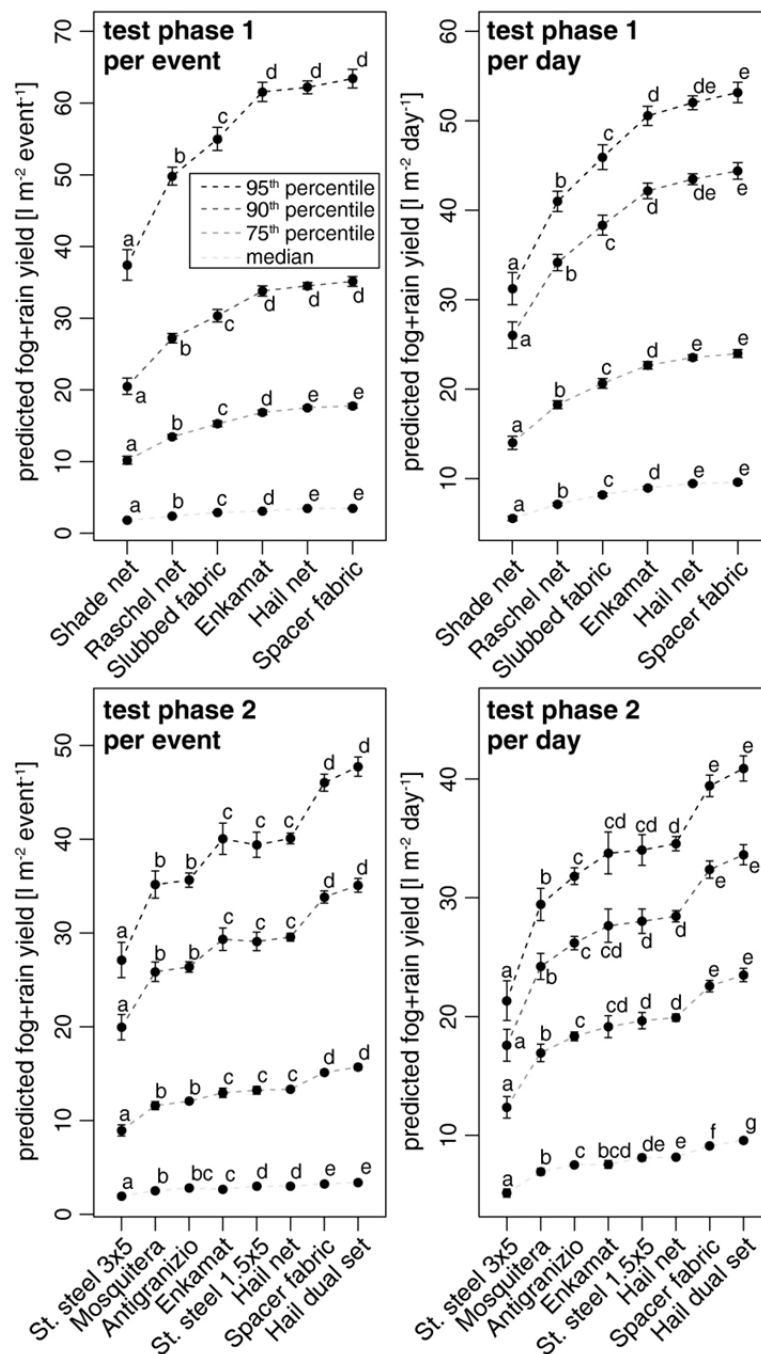


Fig. 5. Influence of mesh type on fog + rain yields. Points show the predicted values of yield for various levels of intensity (mean yield). For each mesh type, the four points denote the expected yield under average conditions (median), under above average intensity (75th percentile), and under two extreme fog conditions denoted by the 90th and 95th percentiles. Results are based on linear modelling of fog + rain yield in dependence of fog intensity, but not accounting for mesh position. Different letters indicate significantly different fog yields of nets at $p < 0.05$, with p -values adjusted for multiple testing.

In test phase 1 and for events, the woven fabrics Shade and Raschel net produced the lowest amount of water, with the Shade mesh significantly inferior to the Raschel. Nevertheless, it remains somewhat surprising that the scientifically investigated (Schemenauer and Joe, 1989) and recommended (Schemenauer and Cereceda, 1994a, b)

Raschel mesh is inferior to all monofilaments in test phase 1. Both Shanyengana *et al.* (2003) and Fernandez *et al.* (2016) showed a generally superior yield of the Raschel mesh to five other woven fabrics and a hydrophobically chemically coated metallic mesh, respectively. However, Feld *et al.* (2016) also reported substantially higher (62%

to 178%) yield of Enkamat meshes as compared to Raschel. They also pointed out that based on hydrodynamic theory (Rivera, 2011; Park *et al.*, 2013), their smaller fiber radius and higher mesh fiber spacing is consistent with greater collection efficiencies. The comparably lower Raschel yields in our study may be partly explained by the rigid supporting grid to which the meshes are connected at regular intervals. This almost completely prevents any movement of the Raschel mesh and its two layers (i.e., only the combination of supporting grid with attached mesh layers as a whole will move, but the Raschel layers themselves will not flex or rub against each other), a factor which may enhance the draining in the traditional Raschel/LFC setup (Klemm *et al.*, 2012). In our study, the Slubbed fabric (three-dimensional monofilament) revealed yields ranging between the Raschel and a group of three other monofilament meshes (Enkamat, Hail net and Spacer fabric), which amongst themselves were not differing significantly at high yields. At the median and 75th percentile of mean yields, Enkamat was shown to be significantly inferior to the Hail net and Spacer fabric. While the three-dimensional meshes tended to have a higher yield than most two-dimensional ones, the two-dimensional Hail net was within the group of best-performing meshes. The analysis of the mesh performance in test phase 1 on a daily basis produced very similar results to the event-based approach. The only difference is that Enkamat and Spacer fabric were found to be significantly different at high (90th and 95th percentiles of mean yield) yields.

In test phase 2, the Shade, Raschel and Slubbed fabric meshes were replaced by two additional monofilaments, Mosquitera and Antigranizio as well as a dual set of the Hail net. After the first sub-period (cf. Table 2), the Mosquitera and Enkamat were again exchanged for two stainless steel meshes with 3×5 and 1.5×5 mm mesh width, respectively. Considering both the event- and daily-based analysis, the dual set of Hail nets as well as the Spacer fabric yielded highest water amounts. For the 50th percentile (median) and the daily analysis, Hail dual set provided a significantly higher yield than Spacer fabric. Hail dual set and Spacer fabric were followed by a group consisting of the single Hail net, Stainless steel 1.5×5 mm and Enkamat meshes for most levels of yield. For the median in the event-based analysis, the latter had a significantly lower yield and thus was not included in the group, whereas in the daily version, the intermediate Stainless steel 1.5×5 mm was similar to both Enkamat and Hail net, while the two themselves differed significantly. The inferior Antigranizio was also not statistically different from Enkamat at median yield for the event-based approach and at all levels of yield for the daily analysis. At the 95th percentile in the latter approach, Antigranizio additionally was in one group with Stainless steel 1.5×5 mm. Significantly lower yield was produced by the Mosquitera mesh in the daily analysis, while it was shown similar to Antigranizio for all yield levels in the event-based assessment. The Stainless steel 3×5 mm showed the worst performance in all cases, being significantly inferior to Mosquitera. At median yield levels in the daily analysis, an additional similarity (Mosquitera to Enkamat) was detected. Once more, there is no clear

differentiation of the performance of two- versus three-dimensional meshes, with an intermediate rank for the three-dimensional Enkamat and high yields for the two versions of the Hail net. While the Enkamat and Hail nets were statistically not different in both test phases 1 and 2 (except for median yields in both test phases and the 75th percentile in test phase 1), a significant difference existed between the Hail net and Spacer fabric in test phase 2, which was not present in the first phase. This might be due to differences in the combination of nets and positions or to differences in the fog events (e.g., liquid water content, drop size distribution, wind speed and the influence of rain) between the first and second period.

The latter is confirmed when considering Fig. 6, showing the ranking of each net's fog + rain yield for each event/day in the two test phases. The pattern of colors indicates that the relative performance of the meshes is changing from fog event to fog event, despite the general tendencies of mesh performance outlined above.

Water Quality

An excerpt of the water quality results is listed in Table 3. pH values during both the first flush and steady state conditions (measured in a single fog event each) are within the range specified by the WHO and are thus similar to those reported by Gandhidasan and Abualhamayel (2012), Shanyengana *et al.* (2002) and Abdul-Wahab *et al.* (2007b). Schemenauer and Cereceda (1992) and Sträter *et al.* (2010) report much lower (acid) pH values for two Chilean sites.

In line with the findings of Schemenauer and Cereceda (1992) and Sträter *et al.* (2010), also discussed in Klemm *et al.* (2012) and Domen *et al.* (2014), ion and heavy metal concentrations as well as electrical conductivity during the first flush were much higher (for some substances several orders of magnitude) than under steady state conditions. One reason we suspect for this is dry deposition on the meshes during fog-free periods (cf. Schemenauer and Cereceda, 1992; Sträter *et al.*, 2010; Domen *et al.*, 2014), which in our case must have been relatively severe as the previous fog-free period lasted less than seven hours. Another possibility is the evaporation of water remaining on the meshes after a fog event, leading to a concentration of substances contained in it. While the concentrations of nitrate and aluminum exceed WHO guidelines during the first flush, all measured substances are within the guideline limits during steady state conditions. Dilution of first flush in steady state water or a technical separation of the first flush should render the harvested water drinkable from an inorganic perspective at the collector site. This is a great improvement, compared to water from local wells, which show the influence of local agriculture and missing waste water treatment in high nitrate (above WHO guideline) and chloride concentrations, as well as a high electrical conductivity, depending on the well location. However, following Sträter *et al.* (2010), fog water quality should be verified on a regular basis if it is used for domestic purposes. This should include organic and microbiological contamination and samples taken from the storage and distribution system.

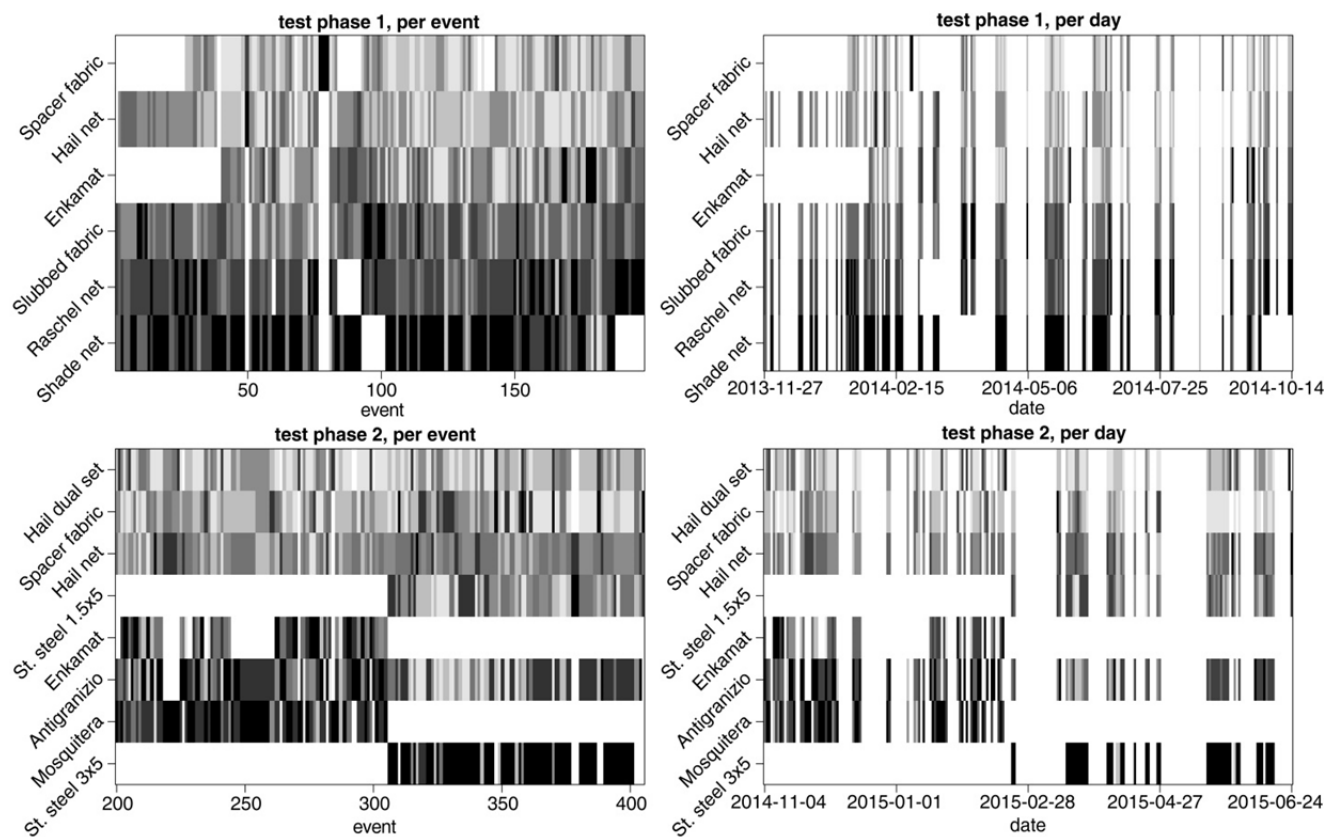


Fig. 6. Ranking of the fog + rain mesh yields per event and per day in test phases 1 and 2. Lighter shades of grey indicate a higher rank; white spaces represent missing data. In case of missing data, ranks were truncated from the high end (i.e., lightest colors are left out).

Differences in water quality between the meshes are generally more pronounced during the first flush than under steady state conditions. This could be caused by different deposition on the diverse mesh structures, but the runoff characteristics and sampling technique may also play an important role, as it governed the sampling process, which was stopped as each sampling bottle was completely full, respectively. Thus, meshes with a faster drainage may have flushed out ions at a faster rate, resulting in less dilution and higher overall concentrations than those found for meshes that do not drain well. These latter meshes (e.g., Enkamat) had to be sampled over a longer time period to obtain the water volume required for the analysis and as a large amount of water is accumulated on the mesh itself, constituents may have been diluted even before any runoff started.

CONCLUSIONS

The novel fog collector presented and investigated here was shown to perform very well within the 19-month study period, without any major mechanical failures of the support structure or any of the tested meshes. While the initial costs for a large-scale application can be expected to be substantially higher than for traditional LFCs, the proposed design is certainly more durable, especially under high wind speeds, and much easier to maintain. In the context of development aid/technical assistance, this can be expected to

lead to a better acceptance and a longer lasting, thus more sustainable, impact of projects.

A fairly clear ranking of the different meshes' yield was determined, with monofilaments generally outperforming the woven fabrics and the Raschel mesh, thus one of the lower-performing options. Apart from the lowest yields represented by two-dimensional meshes, there was no clear differentiation of the performance of two- versus three-dimensional nets, with both options sharing the top (Hail net/Hail net dual set and Spacer fabric, respectively) and lower (Stainless steel 3×5 mm, Mosquitera, Antigranizio and Slubbed fabric, respectively) places in the ranking. While not depending on the position of a mesh inside the linear fog collector, the relative yield and ranking of nets varied considerably from event to event, possibly depending on the wind speed and fog parameters (cf. Park *et al.*, 2013; Fernandez *et al.*, 2016). Overall, highest yields in our study were obtained by the meshes Hail dual set, Spacer fabric and Hail net. While the 'dual set' arrangement requires a significantly higher amount of materials (50% more mesh and twice the amount of supporting grids) and work, the regular Hail net may be interesting for fog harvesting applications as it offers a good balance of yield and costs. The Spacer fabric is generally more expensive; however, it may also be an option as it is now produced commercially and as the cost of the mesh is relatively minor compared to the supporting structure in the presented design.

Table 3. Excerpt of the water quality results. Bold values are outside the WHO guidelines.

Sample	Enkammat	Hail net	Shade net	Slubbed fabric	Spacer fabric	Raschel net	Local wells
<i>pH, WHO guideline: 6.5–9.5</i>							
First flush	7.0	6.7	7.4	7.3	7.2	7.8	7.4–8.2
Steady state	8.4	7.0	7.8	8.5	7.5	8.0	
<i>Electrical conductivity [$\mu\text{S cm}^{-1}$], no WHO guideline</i>							
First flush	360	2,100	1,190	1,710	2,200	1,400	1,070–3,500
Steady state	100	110	114	92	90	108	
<i>Nitrate [mg L^{-1}], WHO guideline: ≤ 50</i>							
First flush	20	200	100	160	210	120	80–280
Steady state	3.5	3.0	3.0	3.0	2.4	3.5	
<i>Ammonium-N [mg L^{-1}], no WHO guideline</i>							
First flush	1.0	4.2	1.2	3.1	5.7	1.5	0.06–0.20
Steady state	1.1	1.0	1.0	1.0	1.0	1.1	
<i>Sulfate [mg L^{-1}], no WHO guideline</i>							
First flush	22	120	68	100	130	85	59–210
Steady state	7.1	7.4	7.4	7.2	6.9	8.4	
<i>Chloride [mg L^{-1}], no WHO guideline</i>							
First flush	87	550	290	440	580	340	210–900
Steady state	24	24	24	23	25	26	
<i>TOC [mg L^{-1}], no WHO guideline</i>							
First flush	3.1	9.1	6.6	9.8	11.0	4.7	1.6–3.7
Steady state	1.6	1.4	1.4	1.2	1.2	1.5	
<i>Aluminum [mg L^{-1}], no WHO guideline</i>							
First flush	0.035	0.110	0.280	0.110	0.094	0.290	< 0.005–0.016
Steady state	0.013	0.022	0.037	0.029	0.011	0.037	
<i>Zinc [mg L^{-1}], no WHO guideline</i>							
First flush	0.070	0.110	0.140	0.230	0.160	0.240	0.0049–0.0360
Steady state	0.045	0.095	0.011	0.026	0.026	0.032	
<i>Manganese [mg L^{-1}], no WHO guideline</i>							
First flush	0.0300	0.1900	0.1200	0.2400	0.2500	0.1900	0.0002–0.0007
Steady state	0.0046	0.0049	0.0042	0.0300	0.0054	0.0071	
<i>Ferrum [mg L^{-1}], no WHO guideline</i>							
First flush	0.0180	0.0820	0.2600	0.0850	0.0400	0.2400	0.0013–0.0074
Steady state	0.0089	0.0160	0.0250	0.0230	0.0081	0.0280	
<i>Selenium [mg L^{-1}], WHO guideline ≤ 0.04</i>							
First flush	0.0019	0.0080	0.0048	0.0072	0.0090	0.0060	0.0073–0.0310
Steady state	0.0010	0.0010	0.0010	0.0010	0.0010	0.0010	
<i>Uranium [mg L^{-1}], WHO guideline ≤ 0.03</i>							
First flush	0.000013	0.000061	0.000120	0.000031	0.000100	0.000069	0.0011–0.0220
Steady state	0.000015	0.000029	0.000025	0.000028	0.000011	0.000018	

Inorganic water quality at the fog collector was acceptable, except for first flush water generated at the start of fog events. This is a first indication that the water may be safe for domestic use, but should be confirmed by further regular measurements, including organic and microbiological contaminations and measurements in the storage and distribution system.

Further scientific studies should include hydrodynamic modelling and laboratory studies of the mesh efficiency with a comparison to the field-based measurements, as well as an investigation of the fog origin, formation and properties and their influence on the relative yield of the meshes. Measuring the droplet sizes and speed classes (e.g., using a fog monitor and/or disdrometer) in the field may also help to accurately separate fog and rain from fog-only events under the conditions experienced in the present study.

For the practical application, setting up and operating a large-scale facility with the novel design and one of the meshes tested will help to further assess the practicability and durability of the design, as well as to accurately calculate the costs and benefits of such an operation. This is currently being done at the study site, using an updated version of the design presented here and the Spacer fabric mesh type.

ACKNOWLEDGMENTS

The authors would like to thank the students Stephan Wunderlich, Simeon Max and Antoine Tranchet for contributing to the project with their Bachelor's theses and study project, respectively. Water analyses were performed free of charge by the Bavarian Authority for Water

Resources Management (Wasserwirtschaftsamt) in Landshut, Germany. Vital, patient and reliable ground support was given by the local Dar Si Hmad staff. Meteorological observations for Guelmim and Sidi Ifni were provided by the website ‘Reliable Prognosis’, rp5.ru. Funding by Munich Re Foundation, Germany is gratefully acknowledged for the pilot facility and scientific investigation.

SUPPLEMENTARY MATERIAL

Supplementary data associated with this article can be found in the online version at <http://www.aaqr.org>.

REFERENCES

- Abdul-Wahab, S.A., Al-Hinai, H., Al-Najar, K.A. and Al-Kalbani, M.S. (2007a). Feasibility of fog water collection. A case study from Oman. *J. Water Supply Res. Technol. AQUA* 56: 275–280.
- Abdul-Wahab, S.A., Al-Hinai, H., Al-Najar, K.A. and Al-Kalbani, M.S. (2007b). Fog water harvesting. Quality of fog water collected for domestic and agricultural use. *Environ. Eng. Sci.* 24: 446–456.
- Azad, M.A.K., Barthlott, W. and Koch, K. (2015a). Hierarchical surface architecture of plants as an inspiration for biomimetic fog collectors. *Langmuir* 50: 13172–13179.
- Azad, M.A.K., Ellerbrok, D., Barthlott, W. and Koch, K. (2015b). Fog collecting biomimetic surfaces: Influence of microstructure and wettability. *Bioinspiration Biomimetics* 10: 016004.
- Bai, F., Wu, J., Gong, G. and Guo, L. (2015). Biomimetic “cactus spine” with hierarchical groove structure for efficient fog collection. *Adv. Sci.* 2: 1500047.
- Bresci, E. (2002). Wake characterization downstream of a fog collector. *Atmos. Res.* 64: 217–225.
- Cao, M., Ju, J., Li, K., Dou, S., Liu, K. and Jiang, L. (2014). Facile and large-scale fabrication of a cactus-inspired continuous fog collector. *Adv. Funct. Mater.* 24: 3235–3240.
- Dodson, L.L. and Bargach, J. (2015). Harvesting fresh water from fog in rural Morocco. Research and impact. Dar Si Hmad’s fogwater project in Aït Baamrane. *Procedia Eng.* 107: 186–193.
- Domen, J.K., Stringfellow, W.T., Camarillo, M.K. and Gulati, S. (2014). Fog water as an alternative and sustainable water resource. *Clean Technol. Environ. Policy* 16: 235–249.
- Dong, H., Zheng, Y., Wang, N., Bai, H., Wang, L., Wu, J., Zhao, Y. and Jiang, L. (2016). Highly efficient fog collection unit by integrating artificial spider silks. *Adv. Mater. Interfac.* 3: 1500831.
- Feld, S.L., Spencer, B.R. and Bolton, S.M. (2016). Improved fog collection using turf reinforcement mats. *J. Sustainable Water Built Environ.* 2: 04016002.
- Fernandez, D., Torregrosa, A., Weiss, P., Cohen, R., Sorensen, D., Kleingartner, J., McKinley, G., Mairs, A., Wilson, S., Bowman, M., Barkley, T. and Gravelle, M. (2016). Inter-mesh comparisons of passive fog collectors. International Conference on Fog, Fog Collection and Dew, Wroclaw, Poland, 24–29 July.
- Gandhidasan, P. and Abualhamayel, H.I. (2012). Exploring fog water harvesting potential and quality in the Asir region, Kingdom of Saudi Arabia. *Pure Appl. Geophys.* 169: 1019–1036.
- Heng, X. and Luo, C. (2014). Bioinspired plate-based fog collectors. *ACS Appl. Mater. Interfaces* 6: 16257–16266.
- Heng, X., Xiang, M., Lu, Z. and Luo, C. (2014). Branched ZnO wire structures for water collection inspired by cacti. *ACS Appl. Mater. Interfaces* 6: 8032–8041.
- Højsgaard, S., Halekoh, U., Robison-Cox, J., Wright, K. and Leidi, A.A. (2013). doBy: doBy - groupwise summary statistics, LSmeans, general linear contrasts, various utilities. R package version 4.5-10. <http://CRAN.R-project.org/package=doBy>, Last Access: 22 November 2016.
- Holmes, R., Rivera, J.D. and Jara, E. (2015). Large fog collectors: New strategies for collection efficiency and structural response to wind pressure. *Atmos. Res.* 151: 236–249.
- Ju, J., Yao, X., Yang, S., Wang, L., Sun, R., He, Y. and Jiang, L. (2014). Cactus stem inspired cone-arrayed surfaces for efficient fog collection. *Adv. Funct. Mater.* 24: 6933–6938.
- Klemm, O., Schemenauer, R.S., Lummerich, A., Cereceda, P., Marzol, V., Corell, D., van Heerden, J., Reinhard, D., Gherezghiher, T., Olivier, J., Osses, P., Sarsour, J., Frost, E., Estrela, M.J., Valiente, J.A. and Fessehaye, G.M. (2012). Fog as a fresh-water resource: Overview and perspectives. *AMBIO* 41: 221–234.
- Lenth, R. (2015). lsmeans: least-squares means. R package version 2.20-23. <http://CRAN.R-project.org/package=lsmeans>, Last Access: 22 November 2016.
- Lummerich, A. and Tiedemann, K.J. (2011). Fog water harvesting on the verge of economic competitiveness. *Erdkunde* 65: 305–306.
- Marzol, M.V. and Megía, J.L.S. (2008). Fog water harvesting in Ifni, Morocco. An assessment of potential and demand. *Die Erde* 139: 97–119.
- Marzol, M.V., Sánchez, J.L. and Yanes, A. (2011). Meteorological patterns and fog water collection in Morocco and the Canary Islands. *Erdkunde* 65: 291–303.
- Park, K.C., Chhatre, S.S., Srinivasan, S., Cohen, R.E. and McKinley, G.H. (2013). Optimal design of permeable fiber network structures for fog harvesting. *Langmuir* 29: 13269–13277.
- Parker, A.R. and Lawrence, C.R. (2001). Water capture by a desert beetle. *Nature* 414: 33–34.
- Pinheiro, J., Bates, D., DebRoy, S., Sarkar, D. and R Core Team (2017). nlme: Linear and Nonlinear Mixed Effects Models. R package version 3.1-131, <https://CRAN.R-project.org/package=nlme>, Last Access: 12.04.2017.
- R Core Team (2014). R: A language for statistical computing. R Foundation for Statistical Computing. Vienna, Austria. <http://www.R-project.org/>, Last Access: 22 November 2016.
- Rivera, J.D. (2011). Aerodynamic collection efficiency of

- fog water collectors. *Atmos. Res.* 102: 335–342.
- Rivera, J.D. and Lopez-Garcia, D. (2015). Mechanical characteristics of Raschel mesh and their application to the design of large fog collectors. *Atmos. Res.* 151: 250–258.
- Schemenauer, R.S. and Joe, P.I. (1989). The collection efficiency of a massive fog collector. *Atmos. Res.* 24: 53–69.
- Schemenauer, R.S. and Cereceda, P. (1992). The quality of fog water collected for domestic and agricultural use in Chile. *J. Appl. Meteorol.* 31: 275–290.
- Schemenauer, R.S. and Cereceda, P. (1994a). A proposed standard fog collector for use in high-elevation regions. *Journal of Appl. Meteorol.* 33: 1313–1322.
- Schemenauer, R.S. and Cereceda, P. (1994b). Fog collection's role in water planning for developing countries. *Nat. Resour. Forum* 18: 91–100.
- Schemenauer, R.S. and Cereceda, P. (1994c). The role of wind in rainwater catchment and fog collection. *Water Int.* 19: 70–76.
- Shanyengana, E.S., Henschel, J.R., Seely, M.K. and Sanderson, R.D. (2002). Exploring fog as a supplementary water source in Namibia. *Atmos. Res.* 64: 251–259.
- Shanyengana, E.S., Sanderson, R.D., Seely, M.K. and Schemenauer, R.S. (2003). Testing greenhouse shade nets in collection of fog for water supply. *J. Water Supply Res. Technol. AQUA* 52: 237–241.
- Sontag, D.S. and Saylor, J.R. (2016). An experimental study of the collection of fog droplets using a mesh fabric: Possible application to cooling towers. *J. Energ. Resour.-ASME* 138: 024501.
- Sträter, E., Westbeld, A. and Klemm, O. (2010). Pollution in coastal fog at Alto Patache, Northern Chile. *Environ. Sci. Pollut. Res.* 17: 1563–1573.
- Tan, X., Shi, T., Tang, Z., Sun, B., Du, L., Peng, Z. and Liao, G. (2016). Investigation of fog collection on cactus-inspired structures. *J. Bionic Eng.* 13: 364–372.
- Wang, Y., Zhang, L., Wu, J., Hedhili, M.N. and Wang, P. (2015). A facile strategy for the fabrication of a bioinspired hydrophilic-superhydrophobic patterned surface for highly efficient fog-harvesting. *J. Mater. Chem. A* 3: 18963–18969.
- Wang, Y., Wang, X., Lai, C., Hu, H., Kong, Y., Fei, B. and Xin, J.H. (2016). Biomimetic water-collecting fabric with light-induced superhydrophilic bumps. *ACS Appl. Mater. Interfaces* 8: 2950–2960.
- Wasserstiftung (2015). Nebelkollector (in German). Utility model DE 20 2014 105 100 U1. <https://register.dpma.de/DPMAregister/pat/PatSchrifteneinsicht?docId=DE202014105100U1>, Last Access: 10 April 2017.
- WHO (2011). *Guidelines for drinking-water quality* - 4th edition. World Health Organization, Geneva. ISBN: 978 92 4 154815 1. 564 pp.
- Wickham, H. (2011). The split-apply-combine strategy for data analysis. *J. Stat. Soft.* 40: 1–29.
- Zheng, Y., Bai, H., Huang, Z., Tian, X., Nie, F.Q., Zhao, Y., Zahi, J. and Jiang, L. (2010). Directional water collection on wetted spider silk. *Nature* 463: 640–643.
- Zhu, H. and Guo, Z. (2016). Hybrid engineered materials with high water-collecting efficiency inspired by Namib Desert beetles. *Chem. Commun.* 52: 6809–6812.
- Zhu, H., Guo, Z. and Liu, W. (2016). Biomimetic water-collecting materials inspired by nature. *Chem. Commun.* 52: 3863–3879.

Received for review, December 1, 2016

Revised, October 9, 2017

Accepted, October 11, 2017